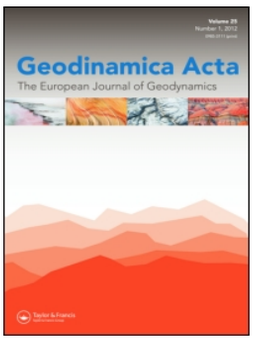

Geodinamica Acta

ISSN: 0985-3111 (Print) 1778-3593 (Online) Journal homepage: https://www.tandfonline.com/loi/tgda20

Evolution of Çamlık fissure-ridge travertines in the Başkale basin (Van, Eastern Anatolia)

Azad Sağlam Selçuk, M. Korhan Erturaç, Serkan Üner, Erman Özsayın & Edwige Pons-Branchu

To cite this article: Azad Sağlam Selçuk, M. Korhan Erturaç, Serkan Üner, Erman Özsayın & Edwige Pons-Branchu (2017) Evolution of Çamlık fissure-ridge travertines in the Başkale basin (Van, Eastern Anatolia), Geodinamica Acta, 29:1, 1-19, DOI: 10.1080/09853111.2016.1228037

To link to this article: https://doi.org/10.1080/09853111.2016.1228037

Accepted author version posted online: 26 Aug 2016.
Published online: 12 Sep 2016.

Geodinamica Acta, 2017
Vol. 29, No. 1, 1–19, https://doi.org/10.1080/09853111.2016.1228037

Evolution of Çamlık fissure-ridge travertines in the Başkale basin (Van, Eastern Anatolia)

Azad Sağlam Selçuk[a]*, M. Korhan Erturaç[b], Serkan Üner[a], Erman Özsayın[c] and Edwige Pons-Branchu[d]

[a]*Department of Geological Engineering, YüzüncüYıl University, Van TR-65100,Turkey;* [b]*Department of Geography, Sakarya University, Sakarya, Turkey;* [c]*Department of Geological Engineering, Hacettepe University, Ankara, Turkey;* [d]*Laboratoire des Sciences du Climat et de l'Environnement (LSCE: UMR CEA/CNRS/UVSQ), Gif-sur-Yvette, France*

(*Received 22 February 2016; accepted 21 August 2016*)

Fissure-ridge travertines (FRTs) are of great importance for the determination and comparison of tectonic deformation in a region. The coeval development of these travertines with active fault zones supplies significant information about regional dynamics in terms of deformation pattern and evolution. In this paper, the characteristics of FRTs of the Başkale basin (eastern Turkey) and responsible regional tectonism are discussed for the first time. The Başkale basin is located between the Başkale Fault Zone (BFZ) characterised by Çamlık fault and Işıklı–Ziraniş fault. It is located between dextral Yüksekova Fault Zone and southern end of dextral Guilato–Siahcheshmeh–Khoy Fault system (Iran). Various morphological features indicating recent activity are exposed along the BFZ, including offsetting rivers, fissure-ridge travertine and fault scarps. The Çamlık fissure-ridge travertine composing of three different depositions is observed along the eastern edge of the BFZ with approximately parallel orientations. The Çamlık fissure-ridge travertine has been formed and developed on fault zone related to strike-slip or oblique movements. We explain how kinematic changes of faults can influence the fissure-ridge development.

Keywords: fissure-ridge travertine; oblique fault; Başkale basin; Turkish–Iran Plateau; Eastern Anatolia

1. Introduction

Travertines are defined as calcium carbonate deposits that form in hydrothermal hot springs and in swamps. If faulting affects areas that are characterised by geothermal anomalies supporting hydrothermal systems, then any damage to the bedrock will give rise to a network of connected fractures. This enhances the permeability of the rock masses, promoting circulation and upwelling of hydrothermal fluids (Bellani, Brogi, Lazzarotto, Liotta, & Ranalli, 2004; Rowland & Sibson, 2004; Sibson, 2000) and further seismic activity (Becken & Ritter, 2012; Becken, Ritter, Bedrosian, & Weckmann, 2011; Gratier, Favreau, Renard, & Pili, 2002). In such cases, the most important factor causing hydrothermal fluids to rise to the surface is the presence of tectonic discontinuity planes such as faults and major joints. Thus, travertines that are deposited by thermal springs can be used as an indicator of tectonic activity (Altunel, 1994; Altunel & Hancock, 1993a, 1993b; Atabey, 2002; Hancock, Chalmers, Altunel, & Çakir, 1999), and their location, age and geometry can assist in understanding geometry and kinematics of the main tectonic structure and stress field (Altunel & Hancock, 1993a, 1993b; Brogi & Capezzuoli, 2009; Faccenna, Funiciello, Montone, Parotto, & Voltaggio, 1993; Hancock et al., 1999; Martinez-Diaz & Hernandez-Enrile, 2001; Temiz & Eikenberg, 2011).

Analysis of fissure-type travertine ridges has been widely used in studies of active tectonics and several fissure-ridges described around the world (Altunel & Hancock, 1993a, 1993b, 1996; Altunel & Karabacak, 2005; Atabey, 2002; Brogi & Capezzuoli, 2009; Brogi, Capezzuoli, Alçiçek, & Gandin, 2014; Brogia et al., 2016; Çakir, 1999; De Filippis & Billi, 2012; De Filippis et al., 2012; De Filippis, Anzalone et al. 2013; De Filippis, Faccenna et al. 2013; Guo & Riding, 1999; Mesci, Gürsoy, & Tatar, 2008; Mesci et al., 2013; Selim & Yanık, 2009; Temiz, Gökten, & Eikenberg, 2009; Temiz & Eikenberg, 2011; Yanık, Uz, & Esenli, 2005). Recent studies have investigated the relationship between fissure-ridge travertines (FRTs) and extensional structures, such as normal or transtensional faults (Alciçek & Özkul, 2005; Altunel, 2005; Brogi, Capezzuoli, Buracchi, & Branca, 2012; Hancock et al., 1999; Shipton et al., 2004) The majority of circulation and upwelling of hydrothermal fluids in geothermal areas depend on fault damage zone (Barbier, 2002). Therefore, travertine masses depositing from thermal springs are considered as indicators of recent tectonic activity (Altunel, 1994; Altunel & Hancock, 1993a, 1993b; Atabey, 2002; Hancock et al., 1999). Hancock et al. (1999) suggest the new concept 'Travitonics' in order to stress the relationship between travertine deposits and faulting. Therefore, travertine deposition becomes a very useful tool for locating active and potentially hazardous faults (Brogi et al., 2012). The architecture and layout of travertine deposits can also provide very helpful information on the tectonic setting of several areas, and supply information on the kinematics of structures affecting the bedrock

*Corresponding author. Email: azadsaglam@yyu.edu.tr

(Brogi et al., 2012). Additionally, the age of the travertine is suggested to be used to determine the age of the fault (Altunel, 1994, 2005; Hancock et al., 1999). Moreover, very valuable information on the fault geometry aligns and linkage can be procured by analysing the travertine masses in terms of morphology and distribution (Brogi et al., 2012).

Travertine fissure-ridges form when hot hydrothermal waters ascend through fractures in the bedrock (Altunel, 1994; Altunel & Hancock, 1993a, 1993b; Atabey, 2002; Bargar, 1978; Chafetz & Folk, 1984; Ford & Pedley, 1996; Guo & Riding, 1998, 1999; Hancock et al., 1999; Yanık et al., 2005). They are identifiable as geomorphological structures with a characteristic main crestal fissure (Altunel & Hancock, 1993a, 1993b, 1996; Bargar, 1978; Çakir, 1999; Chafetz & Folk, 1984; De Filippis et al., 2012; Hancock et al., 1999; Uysal et al., 2007, 2009). Their information is mostly related to (1) damage zone of normal or transtensional faults which develop within the hanging walls of normal faults, (2) in step-over zones between fault segments or (3) in the shear zones related to strike-slip to oblique movements (Altunel & Hancock, 1993a, 1993b, 1996; Atabey, 2002; Çakir, 1999; Hancock et al., 1999).

In this paper, we discuss relationship between fissure-ridge travertine (Çamlık fissure-ridge, Başkale, Van) that is developed in the eastern side of a broad Pliocene tectonic depression (Başkale basin). We mapped morphotectonic structures from these sites through aerial imagery analysis (various scales) detailed field surveys for collecting morphometric and structural data while mapping at the 1:500 and larger scales. These data allowed us to investigate that Başkale fault zone (BFZ) can influence the fissure-ridge development. In this paper, we describe the evolution of the fissure-ridge travertine is controlled by fault zone and coincides with evolution of sinistral shear zone.

2. Geological setting

2.1. Regional dynamics

The East Anatolian High Plateau (EAHP), north-western Iran and Caucasus regions together form one of the regions of extensive high elevation range (average ~2 km) along the Alpine–Himalayan Mountain belt and also western Asia (Jackson, 1992; Şengör, Özeren, Genç, & Zor, 2003; Şengör & Yılmaz, 1981). The formation of EAHP started following the northward subduction and closure of the Neotethyan oceanic gateway between the Mediterranean and Indian Oceans during the Middle Miocene and has been linked to extension of the Aegean, rifting of the Red Sea, and the formation of the North and East Anatolian fault systems (Jolivet & Faccenna, 2000). The collusion first leads to crustal thickening in the Eurasian plate (Dewey, Hempton, Kidd, Saroglu, & Şengör, 1986) and then to an extensive magmatism on both Eurasian and Arabian plates (Ekici, Alpaslan, Parlak, & Temel, 2007; Notsu, Fujitani, Ui, Matsuda, & Ercan, 1995; Pearce et al., 1990). The initiation of intracontinental tectonics is evidenced by apatite fission track dating of the exhumation of Bitlis–Zagros thrust belt 18–13 Ma ago (Okay, Zattin, & Cavazza, 2010). Active deformation during the continental collision of this period resulted in the topographical rise of the entire region, due to crustal shortening and thickening (Şaroğlu & Yılmaz, 1986; Yılmaz, Şaroğlu, & Güner, 1987). This thickened crust then contributed to the formation of the North Anatolian and East Anatolian transform faults due to N–S-trending contractional regime that prevailed during the continental collision. The region subsequently adapted to the compressional tectonic regime with E-W-oriented extensions (Yılmaz et al., 1987). As a result, the Eastern Anatolia block also termed as the Eastern Anatolia Compressional Tectonic Block, and its extent has been defined through modelling of long-term GPS measurements (Djamour, Vernant, Nankali, & Tavakoli, 2011; Reilinger et al., 2006). The block has been further divided into three plateaus on the basis of GPS measurements: (1) the Turkish–Iranian plateau; (2) the Lesser Caucasus–Talesh plateau; and (3) the Central Iranian plateau (Djamour et al., 2011; Reilinger et al., 2006, Figure 1(a)).

Eastern Turkey is an area of active continental compression (Figure 1(a)), and this region has been dominated by compressional deformation since Early Pliocene (Dewey et al., 1986; Koçyiğit, Yilmaz, Adamia, & Kuloshvili, 2001; Şaroğlu & Yılmaz, 1986; Şengör & Kidd, 1979; Şengör & Yılmaz, 1981; Yılmaz et al., 1987). Previous works have asserted that the compressional–contractional tectonic regime extended beyond the compression-extension neotectonic regime of the Late Pliocene. An extension rate for the Bitlis–Zagros Suture Zone has been given by Djamour et al. (2011), who report a maximum extension of 1–2 mm/year within the Çaldıran-North Tabriz Fault System. This fault system is dominated by a strike-slip regime, and it was noted by these authors that the extension rate increases eastward in concordance with a decrease in the strike-slip component. Additionally, Reilinger et al. (2006) reported that around 10% of the convergence between the Arabian plate and the relatively stable Eurasian plate is accommodated by lithospheric shortening in the northern part of the collision zone, although no associated extension rates were determined. However, Bağcı (1997) calculated the extension rate of Eastern Anatolia to be 7 mm/year on the basis of fault plane solutions.

The EAHP has a complex tectonic structure and is characterised by a strike-slip faulting-dominated neotectonic regime with related structures (Dhont & Chorowicz, 2006; Koçyiğit et al., 2001), including the Başkale sinistral strike-slip fault zones; the Balıkgölü, Karayazı-Erciş, Çaldıran, and Yüksekova dextral strike-slip fault zones, and the Gürpınar thrust or reverse zault zones (Figure 1(b), Arpat, Şaroğlu, & IZ, 1976; Cisternas et al., 1989; Dhont & Chorowicz, 2006; Horasan & Boztepe-Güney, 2006; Koçyiğit, 1985a, 1985b; Koçyiğit et al., 2001;

Rebaï et al., 1993; Şaroğlu, Emre, & Boray, 1987; Şaroğlu & Yılmaz, 1986). A large number of destructive earthquakes of differing magnitudes have been recorded within this region, both historically and more recently by modern instrumentation. For example, the historical earthquakes in Hayatsdzaron on 7 April 1646, in Hoşap on 8 March 1715 and in Ahlat on 30 May 1880 caused considerable destruction to the city of Van and its surroundings (Ambraseys, 2001; Ambraseys & Finkel, 1995). More recently, the earthquakes of Tutak (*Mw* 6.0) in 1941, Çaldıran (*Mw* 7.3) in 1976 and Van-Tabanlı (*Mw* 7.2) in 2011 suggest that the eastern Turkey remains seismically active.

2.2. *Geological setting of the Başkale basin*

Çamlık fissure ridge is located in the eastern side of the Başkale basin, a tectonic depression related to the BFZ. The Başkale basin represents the central part of a broad tectonic depression about 82-km long and NNE–SSW oriented (Figure 2). Four main geological associations are found in the Başkale basin: (1) Pre-Neogene basement metamorphic rocks, dominated by the marbles and schists of the Paleozoic Bitlis Massif (Boray, 1975; Erdoğan, 1975; Göncüoğlu & Turhan, 1984; Ricou, 1971; Yilmaz, 1971, 1975); (2) Neogene clastic sedimentary and volcanic rocks, including lacustrine limestone and sandstones and basalt-tuffs; (3) Quaternary fluvial and colluvial sediments; and (4) Quaternary travertines (Figure 2). The Quaternary part of the basin trends NE–SW and is bounded by basement rocks on its western and eastern sides except in the northern part of basin bounded by volcanic units to the east. The most stratigraphically and tectonically significant Quaternary formations within the study area are the travertine deposits that crop out on the eastern side of the Başkale basin (Figure 3(a)). The northern part of the eastern side of the basin is characterised by terrace-type travertines, while the southern part hosts FRTs.

The margin of the Başkale basin is bounded by NNE–SSW striking sinistral strike-slip fault known as the BFZ. The BFZ itself is around 12-km wide, 100-km long and represents a N–S-trending zone of active deformation located between Lake Van to the west and the Turkish–Iranian border to the east (Emre, Doğan, Özalp, & Yıldırım, 2005; Emre et al., 2013; Koçyiğit, 2005, Figure 1(b)). Based on aerial photographs, the BFZ was divided into two faults which are restricting the east and west of Başkale basin (Koçyiğit, 2005) and divided into six individual segments by Emre et al. (2013). The BFZ is divided into three individual segments based on the geometric changes in the strike orientation (Figure 3(a)). These segments are named as Işıklı, Ziraniş and Çamlık.

The western margin of the Başkale basin is bounded by east-dipping, NNW-SSE striking sinistral strike-slip faults with normal component which are namely Işıklı and Ziraniş segments (Figure 3(a)). These segments elongate between Işıklı and Kaşkol villages and have a linear morphological signature (Figure 3(b)). The morphology of the contact reveals that at this particular point the fault is stepping to the east forming at least two fault scarps. The average elevation of the region (3048 m) drops by around 800 m to the flat surface of the basin on western side (Figure 3(b, c)). The Işıklı segment (near the Işıklı Village) is 20 km and elongates from the eastern slopes of Başkale Mountain (3668 m) and Mengene Mountain (3443 m) (Figure 3(c)). Also at this locality, the fault also creates a boundary for the western margin of the Pre-Neogene basement rocks and Quaternary deposits. Sinistral motion of the Işıklı segment is transferred to Ziraniş segment by a left step over the north of Ortayol Village (Figure 3(a)). Additionally, it is noted that there is minor extension resulting in a small-scale depression on basement rocks. Ziraniş segment elongates towards the eastern slopes of Güven Mountain for ~10 km. This segment has an average strike as N20°E and dipping of east.

The eastern margin of the Başkale basin is bounded by Çamlık Fault. This fault elongates as NE–SW, and show strike-slip and/or oblique-slip (rake ranging from 25° to 45°) (Figure 3(d)) movements with left-lateral kinematics (NE–SW-trending Çamlık Fault shows oblique-slip movement (rake ranging from 25° to 45°) with left-lateral kinematics (Figure 3(d)). The most stratigraphically and tectonically significant Quaternary formations within the study area are the travertine deposits that crop out of along the east side of Başkale basin (Figure 3(d)).

3. Fissure-ridge travertines

FRTs are identifiable as geomorphological structures that occur along the long axes of thermal travertine anticlines, and range from a few tens of metres to over 2000 m in length, with a characteristic main crestal fissure (Altunel & Hancock, 1993a, 1993b, 1996; Bargar, 1978; Çakir, 1999; Chafetz & Folk, 1984; De Filippis et al., 2012; Hancock et al., 1999; Uysal et al., 2007, 2009). Fissure-ridge travertine structures typically contain two dominant deposit types: (1) bedded travertines, which are porous and stratified deposits forming the bulk and flanks of the fissure ridge; and (2) banded travertines, which are sparitic, nonporous and often subvertical deposits, with growth bands of different colours, filling veins that permeate the interior of the bedded travertine (De Filippis, Faccenna et al. 2013). In studying their growth, a number of researchers have suggested that coeval deposition of banded and bedded travertines is tectonically controlled and is related to the progressive dilation of the ridge (Altunel & Hancock, 1993a, 1993b; Çakır, 1999; Mesci et al., 2008; Temiz & Eikenberg, 2011). In contrast, other workers have suggested that the banded and bedded travertines were deposited at different times, owing to the combined effects of climate, local subsidence and the gravitational collapse of the ridge (De Filippis, Anzalone et al. 2013; De Filippis,

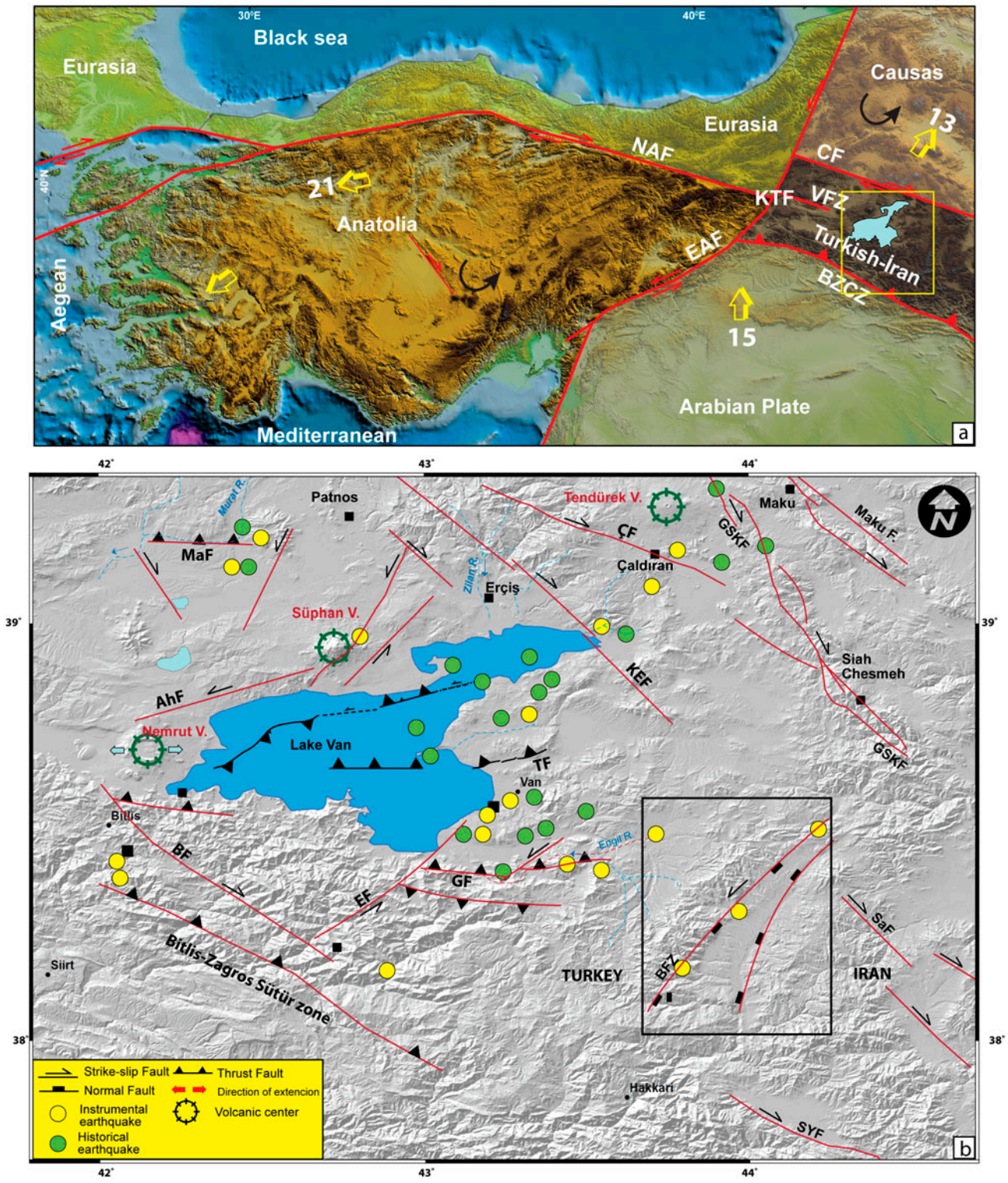

Figure 1. (a) Location of the study area and block boundaries from Reilinger et al. (2006) and Djamour et al. (2011). (b) Seismotectonic map of Lake Van Basin and its surroundings (fault from Karakhanian et al., 2004; Koçyiğit et al., 2001) (earthqukae from Ambraseys & Finkel, 1995; Ergin, Güçlü, & Uz, 1967; Soysal, Sipahioğlu, Kolcak, & Altınok, 1981; Tan, Tapırdamaz, & Yörük, 2008).

Faccenna et al. 2013). Recent studies have shown that the banded–bedded travertine relationship can be a useful tool in reconstructing the tectonic activity of a region (Brogi et al., 2014).

Various studies from the last 30 years have provided travertine ages of up to 380,000 years, using the $^{230}Th/^{234,238}U$ disequilibrium method (Blackwell & Schwarcz, 1986; Brunnacker, Jäger, Hennig, Preuss, &

Grün, 1983; Eikenberg et al., 2001; Harmon, Głazek, & Nowak, 1980; Schwarcz, Grün, Latham, Mania, & Brunnacker, 1988). The fact that the age of travertines determined represents a valuable opportunity for understanding various problematic tectonic regimes, because travertines typically contain tectonic structures that formed at the time of deposition and shortly thereafter. These preserved structures can provide information on the direction and chronology of the tectonic stress field during and after travertine deposition (Altunel, 1994). As a result, various studies have been conducted to determine the compression directions and dilation rates within a region, based on the information obtained from fissure-ridge travertine deposits (Altunel & Karabacak, 2005; Mesci et al., 2008; Temiz & Eikenberg, 2011; Temiz et al., 2009).

3.1. Çamlık travertine

Pleistocene–Holocene travertines in Başkale basin have been morphological described by Koçyiğit (2005). This travertine was deposited during Pleistocene and Holocene by hot waters and overlies Quaternary fluvio-lacustrine deposits. The variety of travertine outcrop at this region: fissure ridges, terraced mounds, cones and waterfall deposits. The different type travertine and thermal springs are mainly related to the BFZ and intensively located at the east of Başkale basin.

The Çamlık FRTs are located on the eastern side of Başkale basin (Figure 3(a)). This morphotectonic feature is located on a fluvial terrace linked to the morphological evolution induced by the Çığılsu River, running about 500-m west of the study area (Figure 4(a)). The Çamlık FRTs includes three different fissure-ridge travertine with a variety of long and wide (Figure 4(b)). The FRTs within the central fissures are partially filled with banded travertines with NW-SE orientations (Figure 4(b)). Bedded travertines make up the slopes of the FRTs, and vary between 5° and 30° dip angle, with the greatest dip found in the middle of the FRTs (Figure 4(c)). The geometric and morphological features of the fissure ridge are very different to each other. These differences will be discussed in following sections. All of the data (for example: long axis, with) from fissure-ridge travertines are collected by Differential Global Positioning System (DGPS) for analysing the morphotectonic features of 17 fissure ridges (Table 1).

3.1.1. Eastern fissure-ridge travertines

The Eastern fissure-ridge travertines (EFRs) are inactive and are the oldest of the travertines in this region (Figure 4(a)). They are located on the eastern ridge of the Çamlık travertine, and are approximately 3-km long and 12-m wide (Figure 4(a) and Table 1). The orientation of the open fracture ranges N10°–15°W, and the opening is around 90–120-cm wide (Figures 4(b), 5(a, b) and Table 1). The banded travertine that fills the open fracture has thicknesses ranging from 50 to 100 cm. The bedded travertine that forms the slopes of the FRT are around 10–12 m in thickness and their dips varies between 5° and 25° (Figure 4(c)). These bedded-travertines contain alternating colours and textures (Figure 5(c)), which are thought to be related with climatic changes in this region. Additionally, they have been show a generally more gentle inclination and dominantly porous fabric which formed by laminar microbialites composed of shrubs and rafts and associated with micritic laminae and lithoclasts (Brogi et al., 2014). It is suggest that this situation characterised by slow flow on microterraced or gently undulating low-angle slopes (Capezzuoli & Gandin, 2005; Gandin & Capezzuoli, 2008). The contacts were much shaped between banded and bedded travertine. Banded travertine formed by onyx-like and white to brown calcite veins of centimetre. The overall morphological structure of the eastern (1) FRTs comprise a central fissure, with banded travertines on both sides, and bedded travertines forming both slopes (Figure 5(a)). This travertine formation displays a symmetric structure with respect to the central fissure.

3.1.2. Central fissure-ridge travertines

The banded travertine and central fissure are not observed in the Central fissure-ridge travertines (CFRs) and only bedded travertine is exposed on the western slope. The FRT is around 1-km long and has a variable width, ranging from 3 m at the head and 5–6 m in the central section (Figure 6(a, b) and Table 1), and the trend

Table 1. Data for fissure ridges from 1EFR, 2CFR and 3WFR.

Fissure ridge	Lat	Long	Average axis orientation (°)	Length (m)	Width (m)	Height (m)	Master normal fault striking (°)
EFRa	N 37°57′10.80″	E 44°06′20.69″	10	1750	12	10	10
EFRb	N 37°56′10.44″	E 44°06′14.24″	15	1200	8	12	10
CFRa	N 37°56′28.77″	E 44°05′43.96″	22	450	3	5	10
CFRb	N 37°56′53.37″	E 44°05′27.49″	30	470	5	4	10
WFRa	N 37°56′45.40″	E 44°05′23.21″	37	300	2	2	10
WFRb	N 37°56′29.20″	E 44°05′38.04″	45	525	3.5	3	10

of the inactive central fissure varies between N20°W and N30°W (Figure 4(b)). The western slope of bedded travertine, which is used as an onyx mine, is 5–6-m thick and its dips varies between 25° and 35° (Figures 4(c) and 6(c)). The close to black coloured bands of travertine are seen in the alternations of the bedded travertine (Figure 6(c, d)), which indicate sudden chemical changes in the waters that supplied the FRTs. Eastern slope of this travertine is steeper than western slope, creating an asymmetry with respect to the central fissure (Figure 6(a)).

3.1.3. *Western fissure-ridge travertines*

The Western fissure-ridge travertines (WFR) is the youngest of its type in the Başkale basin, and was active until 2014. Thus, it represents a key example of the natural appearance of terraced-mound travertines, whose formation is ongoing on the western slope (Figure 7(a, b)). The WFR is 800-m long and 3–4-m wide along its length (Table 1 and Figure 7(a, b)).The central fissure has width around 20–40 cm (Figure 7(c)) and its orientation varies between N35°W and N45°W (Figure 4(b)). When the open fissure is followed along the ridge, it shows considerable variation in its strike, which indicates that the fissure ridge is affected by intense deformation. Additionally, a number of travertine pools were observed on the ridge, which remained active up to 2014 (Figure 7(c)), but had dried up by 2015 (Figure 7(d)). The overall morphology of the western WFR comprises a central fissure, banded travertines on both sides of the central fissure and bedded travertines along both of the slopes (Figure 8(a, b)). As seen in cross section (Figure 8(a, b)), the WFR was formed as a result of one phases of fluid upwelling, giving rise to the banded and bedded travertines. Some author suggest that minor fractures have been filled by fibrous calcite crystals that grew in syntaxial mode, like the banded travertine veins (Figure 8(c)), thus suggesting hydrothermal fluid circulation also in the peripheral fracture sets (Brogi et al., 2014). Figure 8(c) shows that this fracture (1. Banded travertine) is totally filled by banded calcite veins. In a few cases, banded veins are locally affected by sub-centimetre vertical offsets with a normal component of movement (Brogi et al., 2014). Bedded travertines of WFR are different of bedded of EFR and composed of irregularly alternating laminae or bands of crystalline and microbial facies (Figure 8(a)). The crystalline crust is mostly located in the eastern of part, higher portion of the ridge, where they show highly inclined bedding.

The Çamlık FRTs are mainly related to the activity BFZ and evaluation of FRTs were strictly influenced by the BFZ. Additionally, Başkale basin is sinistral shear zone which is bounded by Çamlık (CF), Ziraniş and Işıklı faults (IF). The FRTs outcrop along the east side of basin in N10°–50°W orientation among faults that are present in the N10°E orientation and is characterised by a sinistral strike-slip with normal component (Figure 9(a, b)). The various morphological features indicate that Işıklı fault firstly leads to the development of basin. Because, IF was formed steep and high fault scarps (up to 500 m) and sudden breaks in slope at western part of basin (Figure 3(c)). No high and steep scarps have been observed along the Çamlık fault (CF), but travertine deposits, fault scarps (78 m) and thermal spring consist of east of Çığılsu river indicate that CF constitutes one of the active faults in Başkale basin.

3.2. *Fissure-ridge morphotectonic and age of travertine deposits*

A detailed geomorphological study has been carried out according to mainly field observation. We analysed the main morphotectonic data from fissure ridges of EFR, CFR and WFR. All of the data (for example: long axis, with) from FRTs are collected by DGPS for analysing the morphotectonic features of 17 fissure ridges (Table 1). These long axes are plotted in Figure 9(c) to understand their spatial distribution and geometrical relationship with the master fault. We have also plotted the angular separation between the strike of the master fault and the strike of the fissure-ridge long axis ($\Delta\alpha$) versus the length of fissure ridges to understand whether the tectonic control on these structures is dependent on their size (Figure 10). Figure 10 shows a weak (EFR and CFR) and moderate (WFR) parallelism between the normal fault and related fissure ridge, whose orientation is pretty scatter and length appears considerably independent of $\Delta\alpha$.

The extension directions have been determined from the orientation of fibres existing in the banded travertines of vertical fractures (Mohajjel & Taghipour, 2014). Therefore, it is a good indicator for regional extension direction (Altunel & Hancock, 1993a; Altunel & Karabacak, 2005; Çakır, 1999; Mesci et al., 2013; Mohajjel & Taghipour, 2014). The FRTs within the central fissures are partially filled with banded travertines with NW–SE orientations (Figure 4(b)). Bedded travertines make up the slopes of the FRTs, and vary between 5° and 30° dip angle, with the greatest dip found in the middle of the FRT (Figure 4(c)). The major trends of the FRTs are found to be N10°W and N50°W (Figure 4(b)). For ease of further study, the FRTs in the Çamlık travertines are numbered 1–3 from east to west. We plotted long axes and present-day extension (GPS data) in rose diagrams (Figure 9(c)) which show that extension direction of this region is NE–SW stress directions and these long axes are rotated anticlockwise (Figure 9(d)). Also, kinematic data-set (dip of fault plane, slicklines) of Çamlık fault were analysed by using the computational ‘Minimized Shear Stress Variation’ algorithm by Michael (1984) embedded in MyFault© 1.03 (Pangea Scientifi c™) software (Figure 9(a)). There is a good agreement between the kinematic data-sets of Çamlık fault and elongating long axes of fissure-ridge travertine. The calculated stress tensor of these data-sets indicates a sinistral shear zone with a NE–SW extensional, and NW–SE compressional stress regime (Figure 9(d)).

U-series age determination analyses have been compared the age of fissure-ridge travertine. Samples were collected from the ridge wall (Figure 8(c)), in consideration of the fact that the travertine grew from the fissure margins towards the centre of the fissure and are therefore younger in the centres than at the margins. A total of four banded travertine samples were collected from the Çamlık travertines for U-series age determination. These samples consist of two collections search from the EFR and WFR. Banded travertine was not collected from the CFR, because the margin and the centre of the fissure are not seen in this travertine. Figure 8(c) shows the sampling locations. WFR had begun to form 19,210 ± 1.862 years BP (Table 2). For this reason, Çamlık fault has been active since Late Pleistocene.

4. Discussion

The Başkale basin is one of active deformation area in the Eastern Anatolia. This basin bounded by Çamlık, Işıklı and Ziraniş faults. These faults have been described as pure sinistral strike-slip fault up to now (Emre et al., 2013; Koçyiğit, 2005). But, as kinematic and morphologic data indicate that these faults were characterised by a sinistral strike-slip with normal component as fault scarps, sudden slope, rake ranging from 25° to 45°. Additionally, these faults have been controlled the development of Başkale basin and form sinistral shear zone at this region. But, this basin is characterised by an asymmetrical profile showing along the west to east. Its western slope is higher than eastern slope and two steep of fault scarps. The fault scarps are separated by a NNE–SSW morphological lineament. While the west of first fault scarps controlled by Işıklı segment, second fault scarps can be controlled by a transtensional fault which is located between Ortayol and Işıklı Villages. This fault may be a controlled deformation of middle part of sinistral shear zone (Başkale basin).

Fissure-ridge travertine occurring in several parts of the world are mainly related to damage zone of normal or transtensional faults and associated fractures (Altunel & Hancock, 1993a, 1993b; Brogi et al., 2014; Çakir, 1999; Ford & Pedley, 1996**,** Hancock et al., 1999). The Çamlık travertines are located within the NE-trending Başkale basin in eastern Turkey, having developed in association with the fault zone which is controlled at the Başkale basin; they contain three FRTs structures (Figure 4). These travertines crop out within the N10°E-trending sinistral shear zone, and the FRTs are mainly oriented NW–SE (Figures 3(b) and 4(a)). The orientations of the FRTs are seen to vary between N10°W and N50°W (Figure 4(b)), in approximately 10° steps. This turning of the open fracture indicates that the direction of horizontal extension has shifted counterclockwise and NE–SW extensional direction. Additionally, the calculated stress tensor of kinematic data-sets of Çamlık fault indicates a sinistral shear zone with a NE–SW

Table 2. U-Th measurements for fissure travertines in the Başkale basin, eastern Turkey. ($\delta^{234}U = \{(^{234}U/^{238}U)_{activity} - 1\} \times 1000$.

Sample	^{238}U (µg/g)		^{232}Th (ng/g)		$^{234}U_m$		$(^{230}Th/^{232}Th)$		$(^{230}Th/^{238}U)$		Age (kyr BP)		$^{234}U_{(0)}$		Ages* (kyr BP)	
3 c	0.009	0.00001	0.20	0.0002	162.1	1.4	2.77	0.08	0.0187	0.001	1.70	0.06	162.3	1.5	1.14	0.34
3 m	0.003	0.00001	0.33	0.0004	196.9	2.7	5.86	0.08	0.2222	0.003	22.23	0.38	204.2	4.7	19.21	1.86

Ages* are corrected assuming the initial $^{230}Th/^{232}Th$ activity ratio of 0.9 ± 50%. BP stands for 'Before present' (before 1950).

extensional, and NW–SE compressional stress regime. According to this, turning of the open fracture indicates that extension direction in this region is changed E–W up to NE–SW (Figure 9(d)). It could be explained by the developing of new fault in the middle part of the Başkale basin or consequence of kinematics changes of the master fault. The trends of long axis of Quaternary travertine ridges in the Lake Urmia area (Mohajjel & Taghipour, 2014), located immediately to east of our study area represent strong similarities with those observed in the Başkale basin.

The Çamlık travertines contain three different FRT systems, with variable widths of travertines within the central fissures. The ages of samples collected from the centres and margins of the banded travertines in these fissure ridges were determined using the U/Th disequilibrium method (Table 2). However, we were only able to determine the age of the WFR. We found that this travertine had begun to form 19,210 ± 1.862 years BP ago, but deposition has continued until the present day (Figure 8(d)). Field observations indicate that the EFR is older than the other travertines in the area, mostly because the width of the banded travertine and the length of its long axis are greater than elsewhere (Figure 4(a)). Additionally, these data demonstrate that the BFZ has been active since Late Pleistocene.

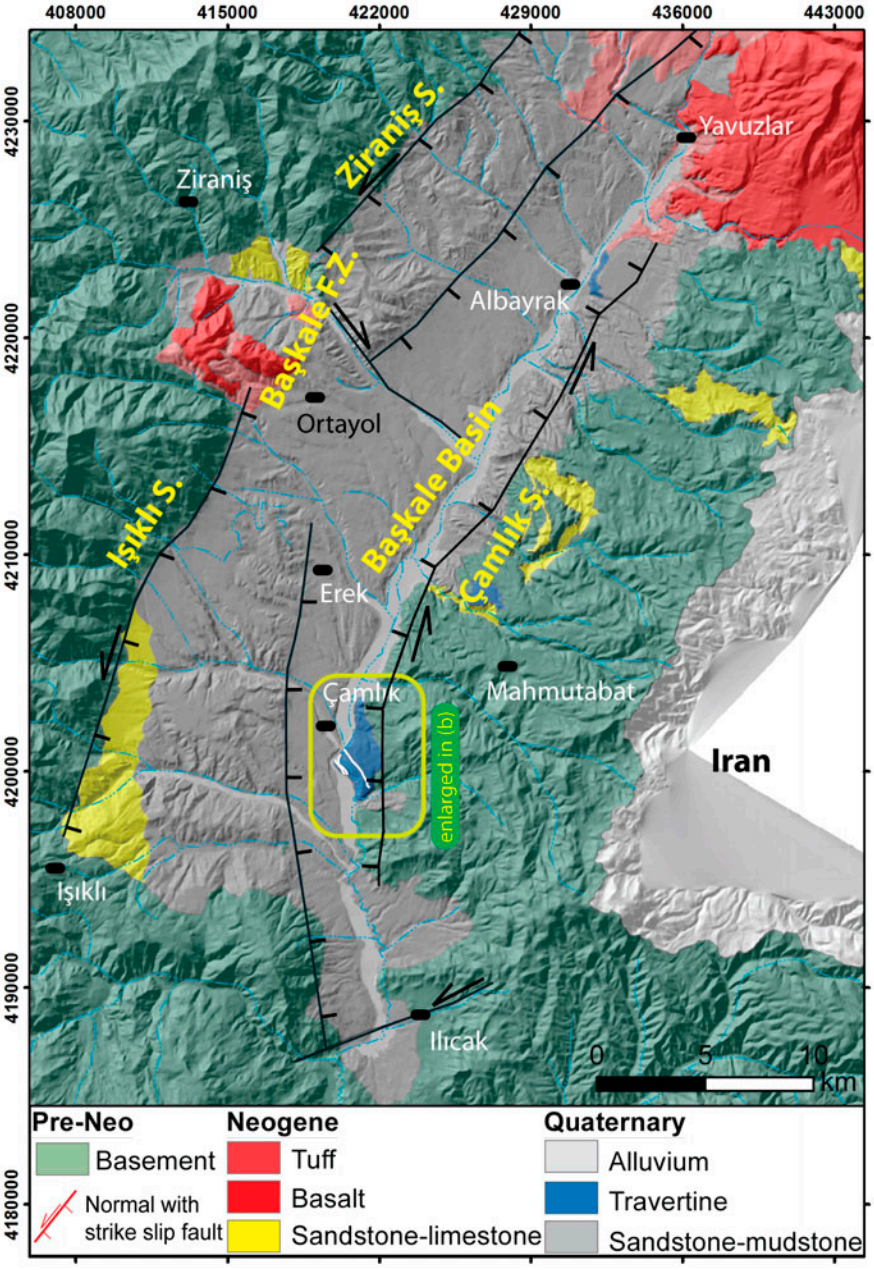

Figure 2. (a) Sketch map of the geology of the Başkale basin (Ateş et al., 2007). (b) Digital elevation model of the study area, including the Çamlık travertine in the Başkale basin.

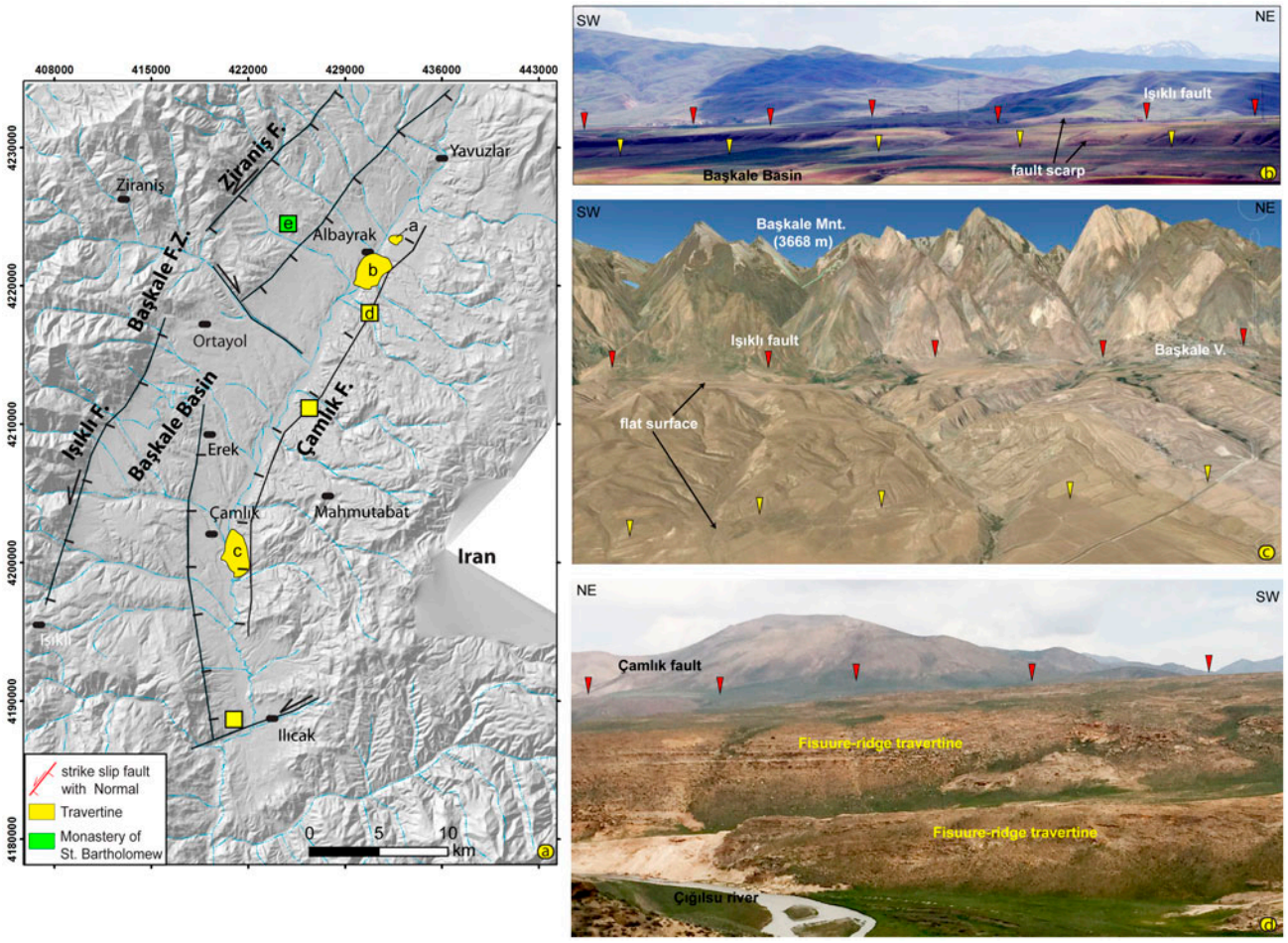

Figure 3. (a) Some of the major active faults in Başkale Basin. (b) Panaromic view of the Işıklı fault the red diamond symbol represents the morphological line of IF. (c) Google Earth™ image showing the detailed geometry of the IF Segment. (d) Panaromic view of the Çamlık fault and Çamlık fissure-ridge travertine.

A further analysis of the obtained FRT ages enables the calculation of dilation rates both during and after the deposition of the fissure ridge (Altunel & Karabacak, 2005; Temiz & Eikenberg, 2011). On the basis of the sampling carried out among the Çamlık travertines of the Başkale basin, we calculated dilation rates of 0.019 mm/year during the deposition of the travertines, and 0.11 mm/year since travertine deposition ceased. Considering this difference in dilation rates, it can be inferred that the extension in this area is non-linear. Further, it can be suggested that the shift in the direction of horizontal extensional stress was the fundamental cause of this discrepancy in dilation rates. Previous studies have estimated extension rates in Eastern Anatolia of 1–2 mm/year on the basis of GPS velocities measured within the Çaldıran-North Tabriz Fault System (Djamour et al., 2011). Our calculations can provide average extensional rates of 0.06 mm/year for the Çamlık travertine in the Başkale basin.

In general, the morphology and internal anatomy of a faulted ridge are strictly influenced by the evolution of the associated fault zone (Brogi et al., 2014). In particular, the morphology and internal anatomy of the Çamlık travertines are excellently preserved (Figure 7(a, b)). Field observations indicate that each of ridges consists of both banded and bedded travertines with no overlap between the individual FRT structures. Even if the WFR uniquely contains two sets of banded and bedded travertines, 1. Banded travertine is actually banded veins and filled by calcite veins. In a few cases, banded veins are locally affected by subcentimetre vertical offsets with a normal component of movement (Brogi et al., 2014). The three FRTs studied here under going progressive migration towards the west (Figure 4(a)) and the elongation of long axis is seen to vary between N10°W and N50°W (Figure 4(b)), in approximately 10° steps. Figure 11 shows the probable evolution of fissure-ridge travertine is influenced by the development of tectonic regime in this region. The basis of field observation, the EFR likely began to develop as a result of movement on the faulting (Figure 11(a)). Probably, transtensional faults in middle of basin have been effective at the development of CFR (Figure 11(b)). As it is seen in cross section at EFR, there is banded calcite vein. This data demonstrate that the Çamlık fault has normal component since Late Pleistocene (Figure 11(c)). All data indicate

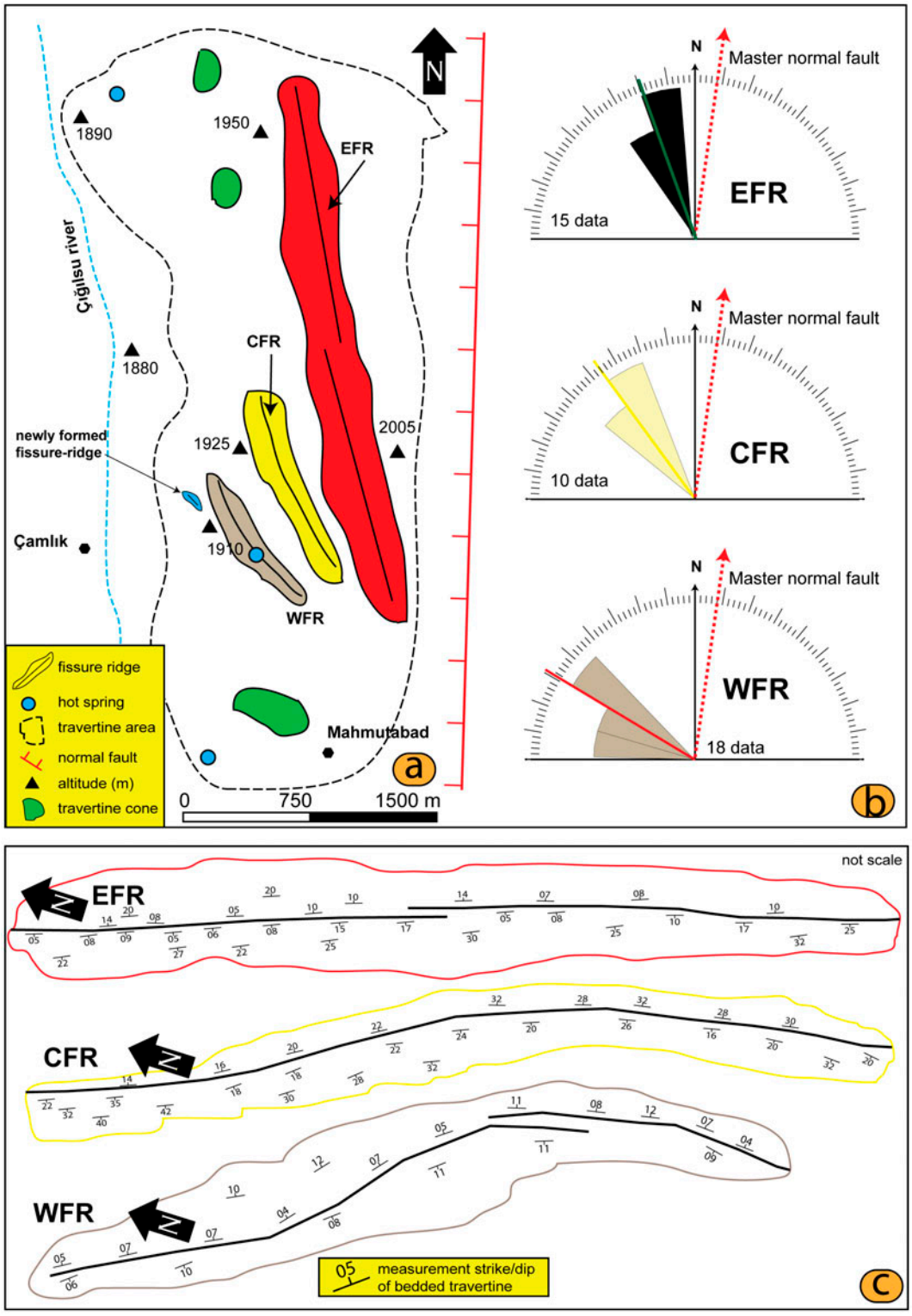

Figure 4. (a) Morphotectonic map for the fissure ridge area of Başkale basin. (b) The rose diagram shows the azimuthal distribution of fissure ridge long axes and the strike of the master normal faults. (c) Strike of the main fissure at the top of the ridge measured at the indicated positions along the fissure ridge.

that growth and development mechanism of the Çamlık fissure-ridge travertine have been influenced by fault zone evolution.

The N–S-trending Başkale basin is located in south-eastern part of the EATCB, and is situated in a critical position for understanding the active deformation of the EATCB itself (Figure 1(b)). The Başkale basin is controlled by the BFZ, and previous studies have suggested that the BFZ shows dominantly sinistral strike-slip movement (Emre et al., 2013; Koçyiğit, 2005). However,

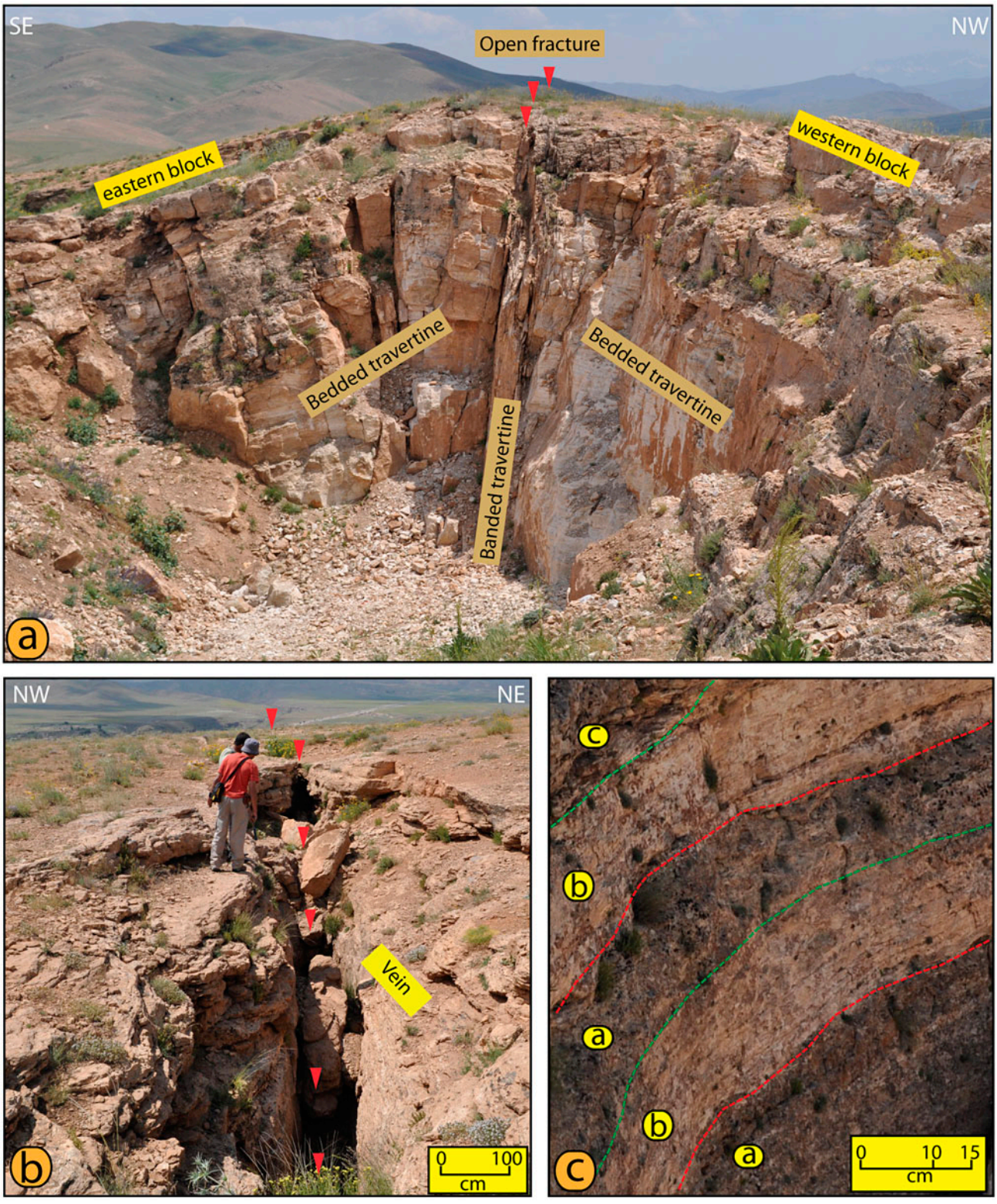

Figure 5. (a) Cross-sectional view of the EFR, showing banded travertines in the central fissure, and bedded travertines in the slope. (b) The central fissure of a ridge. (c) Bedded travertine of the EFR containing alternating colours and textures of travertine.

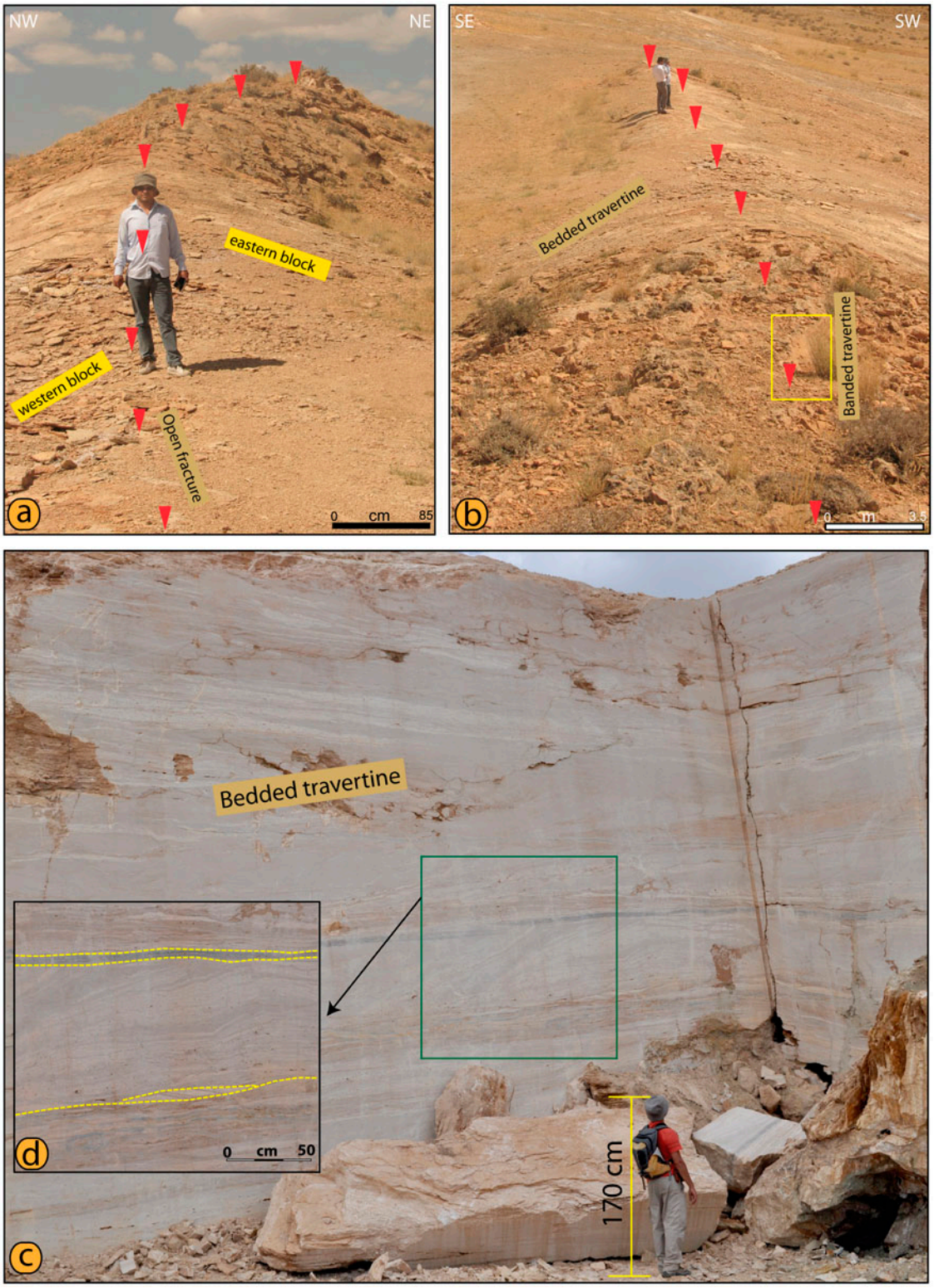

Figure 6. (a, b) Views of the CFR from the top of the ridge. (c) Width of the bedded travertine. (d) Black coloured travertine band within the bedded travertine.

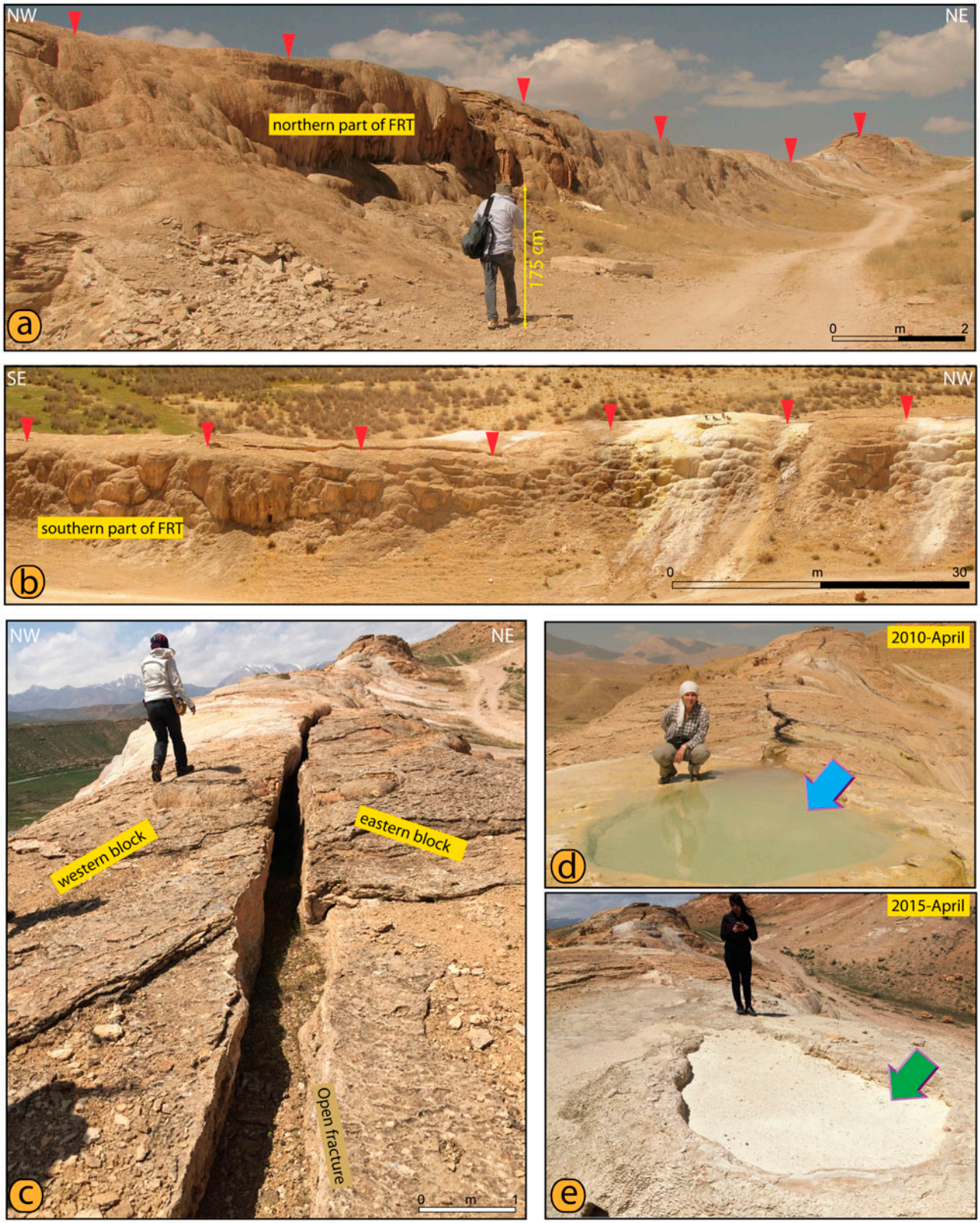

Figure 7. (a, b) Views of the CFR from the top of the ridge. (c) Central fissure of the ridge. (d) Active of travertine pool upon the ridge. (e) Inactive travertine pool upon the ridge.

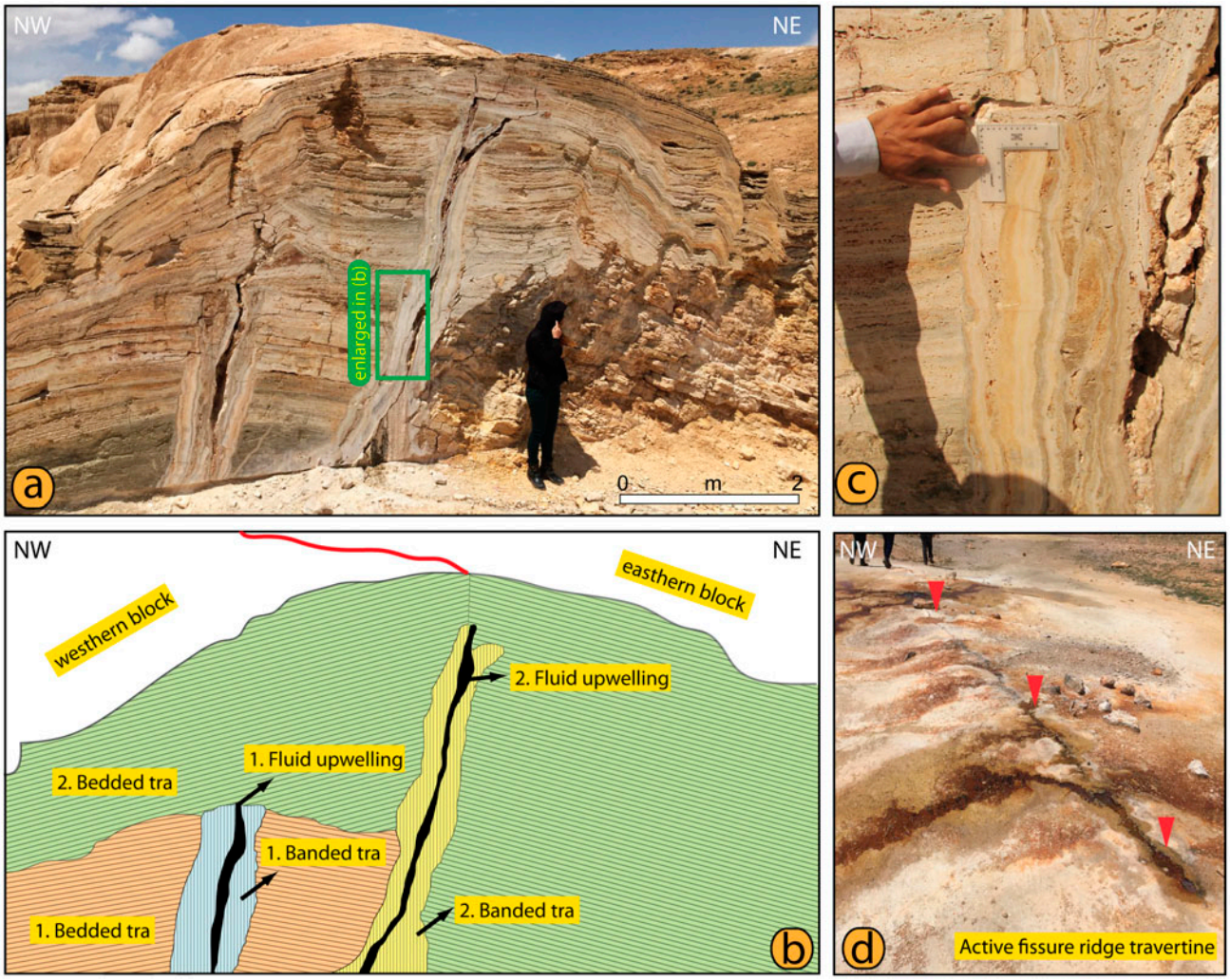

Figure 8. (a) Cross-sectional view of the WFR, containing banded travertines around the central fissure and bedded travertines in the slope. (b) Schematic illustration showing the development of the fissure-ridge travertine. (c) Width of the banded travertine. (d) New fissure-ridge travertine to the west of the existing ridge.

our field studies have shown that the BFZ comprises mostly NNE-trending fault segments, which have sinistral strike-slip movements with a significant normal component (Figure 2).

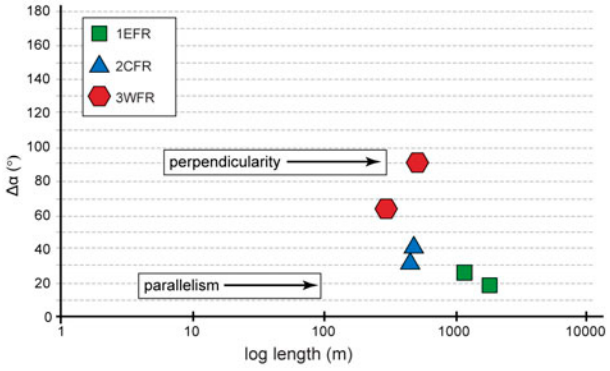

Figure 10. Diagram of Δα versus length of fissure ridges. Δα is the angular separation between the strike of the master normal fault and the strike of fissure ridges.

5. Conclusions

The Çamlık fissure-ridge travertine composing of three different depositions are observed along the eastern edge of the BFZ with approximately parallel orientations. This turning of the open fracture (the slight rotation along the long axis of open fractures) indicates that the direction of horizontal extension has shifted counterclockwise and NE–SW extensional direction. Additionally, kinematic analyses of Çamlık fault indicate NE–SW extensional and NW–SE compressional stress regime in this region. For this reason, there is consistency between extensional direction obtained from kinematic analyses and elongation of long axes of fissure-ridge travertine. However, the plotted elongation of long axes in rose diagrams shows anticlockwise rotation differing between N10°W

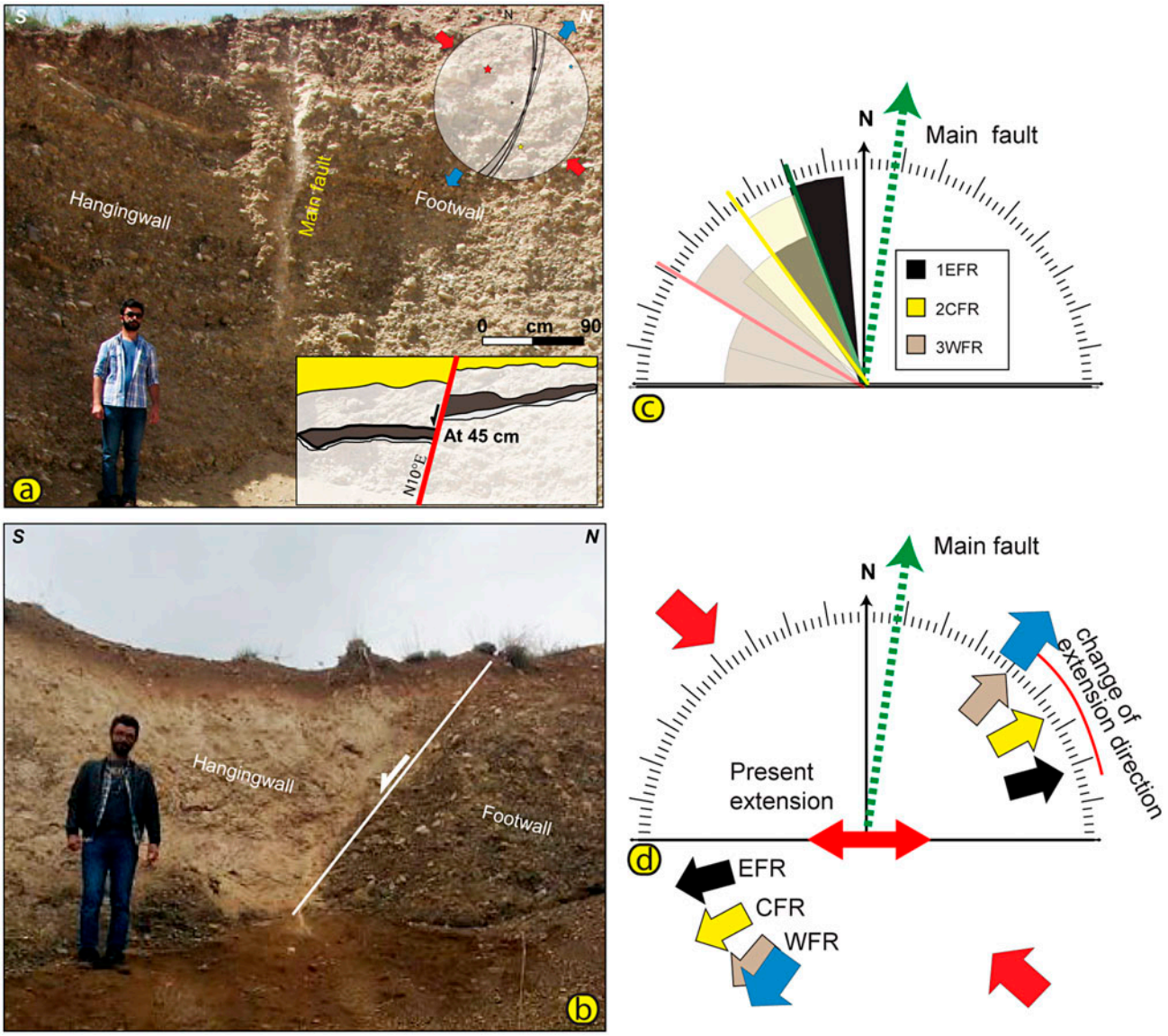

Figure 9. (a) Close-up views of the Çamlık fault and stereographic plots of slip-plane data measured on slickensides of the fault. (b) View of the second fault in Başkale basin. (c) Azimuthal relationship between faults and associated fissure ridges from. Rose diagrams of fissure ridge azimuth for: EFR, CFR and WFR. In the rose diagrams, the direction of present extensions is also plotted. (d) Rose diagrams show stress direction of measured along the Çamlık fault and long axis of FRTs .The Red open arrows the compressional and blue directions extensional directions.

and N50°W (Figure 4(b)), in approximately 10° steps. This causes the anticlockwise rotation was controlled by fault zone evolution. Consequently, the complete developments of the Çamlık fissure-ridge depend on evolution of faults which are bounded Başkale basin and transtensional fault at middle part of this basin.

To understand changes of the tectonic regime in the Eastern Anatolia, the Başkale basin is one of the significant areas of active deformation taking place. This basin is bounded by Çamlık, Işıklı and Ziraniş faults. The kinematic and morphologic data indicate that these faults are characterised by a sinistral strike-slip or with normal component. Various morphological features indicating recent activity are exposed along these faults, including fissure-ridge travertine, sudden break slopes and fault scarps.

Another result of this study is the determination of such dilation rates in the Başkale basin from structural and radiometric analysis of the FRTs; they were found to extend at a rate of 0.019 mm/year during travertine deposition, and 0.11 mm/year after deposition had ceased.

In sum, fissure-ridge travertine developments are affected by tectonic regimes in the region and it carry the traces of the regime change.

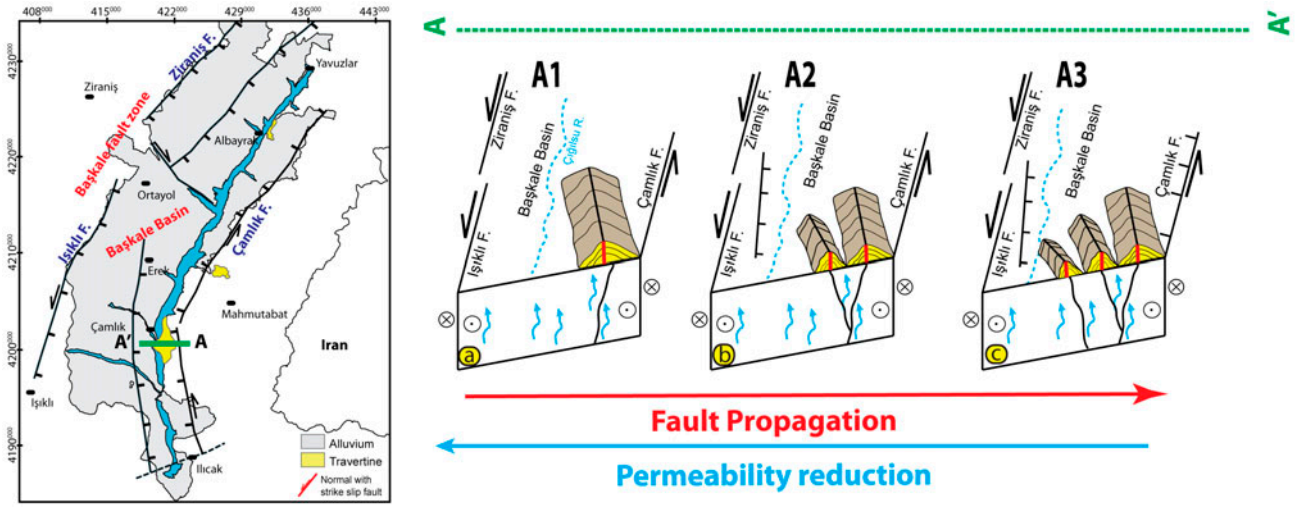

Figure 11. Schematic illustrations, based on our field data, developing of the Çamlık travertine, which is influenced under change of the tectonic regime in Başkale basin, resulting in the progressive migration of the three FRTs.

Acknowledgements

The manuscript was much improved by the constructive critical reviews by reviewers of A. Brogi and by editor of E. Bozkurt. The author is grateful to Uğur Temiz for her help during the organisation of the figures, and to their viewers for their fruitful comments and improvements to the manuscript. The paper was edited for English language by Editage.

Disclosure statement

No potential conflict of interest was reported by the authors.

Funding

This work was financially supported by the Yüzüncü Yıl University Scientific Project [Project Number 2015-MİM-B068].

ORCID

Azad Sağlam Selçuk http://orcid.org/0000-0003-4943-3870
M. Korhan Erturaç http://orcid.org/0000-0002-6501-760X
Serkan Üner http://orcid.org/0000-0001-5974-1856

References

Alciçek, M. C., & Özkul, M. (2005, September 21–25). Extensional faulting induced tufa precipitation in the Neogene C, ameli Basin of south-western Anatolia, Turkey. In M. Ozkul, S. Yagiz, & B. Jones (Eds.), *Travertine, Proceedings of 1st International Symposium on Travertine, Denizli-Turkey* (pp. 120–127). Ankara: Kozan Ofset.

Altunel, E. (1994). *Active tectonics and the evolution of Quaternary travertines at Pamukkale, Western Turkey* (PhD thesis). University of Bristol, Bristol, UK.

Altunel, E. (2005, September 21–25). Travertines: Neotectonic indicators. In M. Ozkul, S. Yagiz, & B. Jones (Eds.), *Travertine, Proceedings of 1st International Symposium on Travertine, Denizli, Turkey* (pp. 120–127). Ankara: Kozan Ofset.

Altunel, E., & Hancock, P. L. (1993a). Active fissuring and faulting in Quaternary travertines at Pamukkale, Western Turkey. *Zeitschrift für Geomorphologie Supplement, 94*, 285–302.

Altunel, E., & Hancock, P. L. (1993b). Morphology and structural setting of Quaternary travertines at Pamukkale, Turkey. *Geological Journal, 28*, 335–346.

Altunel, E., & Hancock, P. L. (1996). Structural attributes of travertine-filled extensional fissures in the Pamukkale Plateau, Western Turkey. *International Geology Review, 38*, 768–777.

Altunel, E., & Karabacak, V. (2005). Determination of horizontal extension from fissure-ridge travertines: A case study from the Denizli Basin, southwestern Turkey. *Geodinamica Acta, 18*, 333–342. doi:10.3166/ga.18.333-342

Ambraseys, N. N. (2001). Reassessment of earthquakes, 1900–1999, in the Eastern Mediterranean and the Middle East. *Geophysical Journal International, 145*, 471–485. doi:10.1046/j.0956-540x.2001.01396.x/epdf

Ambraseys, N. N., & Finkel, C. (1995). *The seismicity of Turkey and adjacent areas. A historical review 1500–1800.* İstanbul: Eren Yayıncılık.

Arpat, E., Şaroğlu, F., & Iz, H. (1976). Çaldıran earthquake. *Yeryuvarı ve İnsan, 2*, 29–41.

Atabey, E. (2002). The formation of fissure ridge type laminated travertine-tufa deposits microscopical characteristics and diagenesis, Kirsehir Central Anatolia. *Mineral Research Exploration Bulletin., 123–124*, 59–65.

Ateş, Ş., Mutlu, G., Özerk, O. Ç., Çiçek, İ., Karakaya Gülmez, F., Bulut Üstün, A., … Aksoy, A. (2007). *Geoscience data of Van Province* (Report No. 10961, p. 152s). General Directorate of Mineral Research and Exploration. (unpublished).

Bağcı, G. (1997). Rates of Crustal deformation in eastern Anatolia. *Geophyics, 11*, 53–64.

Barbier, E. (2002). Geothermal energy and current status: An overview. *Renewable and Sustainable Energy Reviews, 6*, 3–65.

Bargar, K. E. (1978). Geology and thermal history of Mammoth Hot Springs, Yellowstone National Park, Wyoming. *U.S. Geological Survey Bulletin, 1444*, 1–55.

Becken, M., & Ritter, O. (2012). Magnetotelluric studies at the San Andreas fault zone: Implications for the role of fluids. *Surveys in Geophysics, 33*, 65–105. doi:10.1007/s10712-011-9144-0

Becken, M., Ritter, O., Bedrosian, P. A., & Weckmann, U. (2011). Correlation between deep fluids, tremor and creep along the central San Andreas fault. *Nature, 480*, 87–90. doi:10.1038/nature10609

Bellani, S., Brogi, A., Lazzarotto, A., Liotta, D., & Ranalli, G. (2004). Heat flow, deep temperatures and extensional structures in the Larderello geothermal field (Italy): Constraints on geothermal fluid flow. *Journal of Volcanology and Geothermal Research, 132*, 15–29. doi:10.1016/S0377-273(03)00418-9

Blackwell, B., & Schwarcz, H. P. (1986). U-series analyses of the lower travertine at Ehringsdorf. *Quaternary Research, 25*(2), 215–222.

Boray, A. (1975). Bitlis dolayının yapısı ve metamorfizması [Structure and metamorphism of Bitlis]. *Geological Bulletin of Turkey, 18*, 81–84.

Brogi, A., & Capezzuoli, E. (2009). Travertine deposition and faulting: The Faultrelated travertine fissure-ridge at Terme S. Giovanni, Rapolano Terme (Italy). *Geologische Rundschau, 98*, 931–947. doi:10.1007/s00531-007-0290-z

Brogi, A., Capezzuoli, E., Alçiçek, M. C., & Gandin, A. (2014). Evolution of a fault-controlled fissure-ridge type travertine deposit in the western Anatolia extensional province: The Çukurbağ fissure-ridge (Pamukkale, Turkey). *Journal of the Geological Society, 171*(3), 425–441. doi:10.1144/jgs2013-034

Brogi, A., Capezzuoli, E., Buracchi, E., & Branca, M. (2012). Tectonic control on traver-tine and calcareous tufa deposition in a low-temperature geothermal system (Sarteano, Central Italy). *Journal Geological Society of London, 169*, 461–476. doi:10.1144/0016-76492011-137

Brogia, A., Alçiçek, M., Yalçıner, C. Ç., Capezzuoli, E., Liotta, D., Meccheri, M., … Shen, C. C. (2016). Hydrothermal fluids circulation and travertine deposition in an active tectonic setting: Insights from the Kamara geothermal area (western Anatolia, Turkey). *Tectonophysics, 680*, 211–232. doi:10.1016/j.tecto.2016.05.003

Brunnacker, K., Jäger, K. D., Hennig, G. J., Preuss, J., & Grün, R. (1983). Radiometrische Untersuchungen zur Datierung mitteleuropäischer Travertinvorkommen [Audiometric tests for 40 dating Central European travertine deposits]. *Ethnographisch-Archäologische Zeitschrift, 24*, 217–266.

Capezzuoli, E., & Gandin, A. (2005). Facies distribution and microfacies of thermal-spring travertine from Tuscany. In M. Özkul, S. Yagiz, & B. Jones (Eds.), *Proceedings of 1st International Symposium on Travertine, Pamukkale University, Denizli (Tr)* (pp. 43–50). Ankara: Kozan Ofset.

Chafetz, H. S. & Folk, R. L. (1984). Travertines: Depositional morphology and the bacterially constructed constituents. *Journal of Sedimentary Petrology, 54*, 289–316.

Cisternas, A., Philip, H., Bousquet, J. C., Cara, M., Deschamps, A., Dorbath, L., & Tatevossian, R. (1989). The Spitak (Armenia) earthquake of 7 December 1988: Field observations, seismology and tectonics. *Nature, 339*(6227), 675–679. doi:10.1038/339675a0

Çakır, Z. (1999). Along-strike discontinuity of active normal faults and its influence on Quaternary travertine deposition; examples from western Turkey. *Turkish Journal of Earth Sciences, 8*, 67–80.

De Filippis, L., Anzalone, E., Billi, A., Faccenna, C., Poncia, P. P., & Sella, P. (2013). The origin and growth of a recently-active fissure ridge travertine over a seismic fault, Tivoli, Italy. *Geomorphology, 195*, 13–26. doi:10.1016/j.geomorph.2013.04.019

De Filippis, L., & Billi, A. (2012). Morphotectonics of fissure ridge travertines from geothermal areas of Mammoth Hot Springs (Wyoming) and Bridgeport (California). *Tectonophysics, 548–549*, 34–48. doi:10.1016/j.tecto.2012.04.017

De Filippis, L., Faccenna, C., Billi, A., Anzalone, E., Brilli, M., Ozkul, M., & Villa, I. M. (2012). Growth of fissure ridge travertines from geothermal springs of Denizli Basin, western Turkey. *Geological society of America Bulletin, 124*, 1629–1645. doi:10.1130/B30606.1

De Filippis, L., Faccenna, C., Billi, A., Anzalone, E., Brilli, M., Soligo, M., & Tuccimei, P. (2013). Plateau versus fissure ridge travertines from Quaternary geothermal springs of Italy and Turkey: Interactions and feedbacks between fluid discharge, paleoclimate, and tectonics. *Earth-Science Reviews, 123*, 35–52. doi:10.1016/j.earscirev.2013.04.004

Dewey, J. F., Hempton, M. R., Kidd, W. S. F., Saroglu, F., & Şengör, A. M. C. (1986). Shortening of continental lithosphere: The neotectonics of Eastern Anatolia – A young collision zone. *Geological Society Special Publication, 19*, 1–36, doi:10.1144/GSL.SP.1986.019.01.01

Dhont, D., & Chorowicz, J. (2006). Review of the neotectonics of the Eastern Turkish-Armenian Plateau by geomorphic analysis of digital elevation model imagery. *International Journal of Earth Sciences, 95*, 34–49. doi:10.1007/s00531-005-0020-3

Djamour, Y., Vernant, P., Nankali, H. R., & Tavakoli, F. (2011). NW Iran-eastern Turkey present-day kinematics: Results from the Iranian permanent GPS network. *Earth and Planetary Science Letters, 307*, 27–34. doi:10.1016/j.epsl.2011.04.029

Eikenberg, J., Vezzu, G., Zumsteg, I., Bajo, S., Ruethi, M., & Wyssling, G. (2001). Precise two chronometer dating of Pleistocene travertine: The 230Th/234U and 226Raex/226Ra(0) approach. *Quaternary Science Reviews, 20*, 1935–1953. doi:10.1016/S0277-3791(01)00020-8

Ekici, T., Alpaslan, M., Parlak, O., & Temel, A. (2007). Geochemistry of the Pliocene basalts erupted along the Malatya-Ovacık fault zone (MOFZ), Eastern Anatolia, Turkey: Implications for source characteristics and partial melting processes. *Chemie der Erde – Geochemistry, 67*, 201–212.

Emre, Ö., Doğan, A., Özalp, Ö., & Yıldırım, Y., (2005). *25 Ocak 2005 Hakkari Depremi Hakkında Ön Değerlendirme* (Report No. 123). General Directorate of Mineral Research and Exploration, Ankara. [in Turkish]

Emre, Ö., Duman, T. Y., Özalp, S., Elmacı, H., Olgun, Ş., & Şaroğlu, F., (2013). Annotated active fault map of Turkey, 1:1 250 000: *MTA Özel yayınlar serisi*-30, 89s.

Erdoğan, T. (1975). *Gölbaşı Civarının Jeolojisi [Geology of the surrounding Gölbaşı]* (Report No. 929, p. 18). Ankara: Turkish petroleum corporation.

Ergin, K., Güçlü, U., & Uz, Z., (1967). *Earthquake catalogue of Turkey and surrounding (until the end of the 11 years after 1964 BC)* (Vol. 24, p. 169). Ankara: İ.T.Ü., Maden Fak. Supply of Physics Publishing.

Faccenna, C., Funiciello, R., Montone, P., Parotto, M., & Voltaggio, M. (1993). Late Pleistocene strike slip tectonics in the Acque Albule basin (Tivoli, Latium). *Memorie Descrittive della Carta Geologica d'Italia, 69*, 37–50.

Ford, T. D., & Pedley, H. M. (1996). A review of tufa and travertine deposits of the world. *Earth-Science Review, 41*, 17–175. doi:10.1016/S0012-8252(96)00030-X

Gandin, A., & Capezzuoli, E. (2008). Travertine versus calcareous tufa: Distinctive petrologic features and stable isotopes signatures. *Italian Journal of Quaternary Science, 21*, 125–136.

Göncüoğlu, M. C., & Turhan, N. (1984). Geology of the Bitlis metamorphic belt. In O.Tekeli, & M. C.Göncüoğlu (Eds.), *Geology of the Tauraus Belt* (pp. 237–244). Ankara: MTA publications.

Gratier, J. P., Favreau, P., Renard, F., & Pili, E. (2002). Fluid pressure evolution during the earthquake cycle controlled by fluid flow and pressure solution crack sealing. *Earth Planets Space, 54*, 1139–1146.

Guo, L., & Riding, R. (1998). Hot-spring travertine facies and sequences, late Pleistocene, Rapolano Terme, Italy. *Sedimentology, 45*, 163–180. doi:10.1046/j.1365-3091.1998.00141.x

Guo, L., & Riding, R. (1999). Rapid facies changes in Holocene fissure ridge hot spring travertines, Rapolano Terme, Italy. *Sedimentology, 46*, 1145–1158. doi:10.1046/j.1365-3091.1999.00269.x

Hancock, P. L., Chalmers, R. M. L., Altunel, E., & Çakir, Z. (1999). Travitonics: Using travertines in active fault studies. *Journal of Structural Geology, 21*, 903–916. doi:10.1016/S0191-8141(99)00061-9

Harmon, R. S., Głazek, J., & Nowak, K. (1980). 230Th/234U dating of travertine from the Bilzingsleben archaeological site. *Nature, 284*(5752), 132–135.

Horasan, G., & Boztepe-Güney, A. (2006). Observation and analysis of low frequency crustal earthquakes in Lake Van and its vicinity, eastern Turkey. *Journal Seismology, 11*, 1–13. doi:10.1007/s10950-006-9022-2

Jackson, J. (1992). Partitioning of strike-slip and convergent motion between Eurasia and Arabia in eastern Turkey and the Caucasus. *Journal Geophysical Researchers, 97*, 471–479.

Jolivet, L., & Faccenna, C. (2000). Mediterranean extension and the Africa–Eurasia collision. *Tectonics, 19*, 1095–1106.

Karakhanian, A. S., Trifonov, V. G., Philip, H., Avagyan, A., Hessami, K., Jamali, F., … Adilkhanyan, A. (2004). Active faulting and natural hazards in Armenia, eastern Turkey and northwestern Iran. *Tectonophysics, 380*, 189–219. doi:10.1016/j.tecto.2003.09.020

Koçyiğit, A. (1985a). Karayazi fault. *Geological Society of Turkey Bulletin, 28*, 67–72.

Koçyiğit, A. (1985b). Muratbast-Balabantas (Khorasan) between the geotechnical characteristics of the Çobandede fault kusagi and Khorasan-Narman earthquake surface fractures. *Cumhuriyet University Journal of Engineering Faculty Series A-Earth Science, 2*, 17–33.

Koçyiğit, A. (2005). *Sütlüce (Hakkari) supply of earthquake: Başkale fault zone of SE Turkey*. Paper presented at the Eartquake Symposium, Denizli, Turkey.

Koçyiğit, A., Yilmaz, A., Adamia, S., & Kuloshvili, S. (2001). Neotectonic of East Anatolian Plateau (Turkey) and Lesser Caucasus: Implication for transition from thrusting to strike-slip faulting. *Geodinamica Acta, 14*, 177–195. doi:10.1080/09853111.2001.11432443

Martinez-Diaz, J. J., & Hernandez-Enrile, J. L. (2001). Using travertine deformations to characterize paleoseismic activity along an active oblique-slip Fault: The Alhama de Murcia Fault (Betic Cordillera, Spain). *Acta Geologica Hispanica, 36*, 297–313.

Mesci, L. B., Gürsoy, H., & Tatar, O. (2008). The evolution of travertine masses in the Sivas Area (Central Turkey) and their relationships to active tectonics. *Turkish Journal of Earth Sciences, 17*, 219–240.

Mesci, L. B., Tatar, O., Piper, J. D. A., Gürsoy, H., Altunel, E., & Crowley, S. (2013). The efficacy of travertines as a palaeoenvironmental indicator: Palaeomagnetic study of neotectonic examples from Denizli, Turkey. *Turkish Journal of Earth Sciences, 22*, 191–203. doi:10.3906/yer-1112-3

Michael, A. J. (1984). Determination of stress from slip data: Faults and folds. *Journal of Geophysical Research, 89*, 11517–11526.

Mohajjel, M., & Taghipour, K. (2014). Quaternary travertine ridges in the Lake Urmia area: Active extension in NW Iran. *Turkish Journal of Earth Sciences, 23*, 602–614.

Notsu, K., Fujitani, T., Ui, T., Matsuda, J., & Ercan, T. (1995). Geochemical features of collisionrelated volcanic rocks in central and eastern Anatolia. *Journal of Volcanology and Geothermal Research, 64*, 171–191.

Okay, A. I., Zattin, M., & Cavazza, W. (2010). Apatite fission-track data for the Miocene Arabia–Eurasia collision. *Geology, 38*, 35–38.

Pearce, J. A., Bender, J. F., De Long, S. E., Kidd, W. S. F., Low, P. J., Güner, Y., … Mitchell, J. G. (1990). Genesis of collision volcanism in Eastern Anatolia. *Journal of Volcanology and Geothermal Research, 44*, 189–229.

Rebaï, S., Philip, H., Dorbath, L., Borissoff, B., Haessler, H., & Cisternas, A. (1993). Active tectonics in the Lesser Caucasus: Coexistence of compressive and extensional structures. *Tectonics, 12*, 1089–1114. doi:10.1029/93TC00514

Reilinger, R., McClusky, S., Vernant, P., Lawrence, S., Ergintav, S., Cakmak, R., & Stepanyan, R. (2006). GPS constraints on continental deformation in the Africa–Arabia–Eurasia continental collision zone and implications for the dynamics of plate interactions. *Journal of Geophysical Research: Solid Earth (1978–2012), 111*(B5), 1–26. doi:10.1029/2005JB004051

Ricou, L., (1971). Le croissant ophiolitique péri-arabe: Une ceinture de nappes mises en place au Crétacé supérieur [The growing ophiolite perioral: A belt plies in place in the Late Cretaceous]. *Revue de géographie physique et de géologie dynamique, 13*, 327–350.

Rowland, J. V., & Sibson, R. H. (2004). Structural controls on hydrothermal flow in a segmented rift system, Taupo Volcanic Zone, New Zealand. *Geofluids, 4*, 259–283. doi:10.1111/j.1468-8123.2004.00091.x

Schwarcz, H. P., Grün, R., Latham, A. G., Mania, D., & Brunnacker, K. (1988). The Bilzingsleben archaeological site: New dating evidence. *Archaeometry, 30*, 5–17.

Selim, H. H., & Yanık, G. (2009). Development of the Cambazli (Turgutly/Manisa) fissure-ride-type travertine and relationship with active tectonics, Gediz Graben, Turkey. *Quaternary International, 199*, 157–163. doi:10.1016/j.quaint.2008.04.009

Shipton, Z. K., Evans, J. P., Kirschner, D., Kolesar, P. T., Williams, A. P., & Heath, J. E. (2004). Analysis of CO_2 leakage through "low-permeability" fault from natural reservoirs in the Colorado Plateau, southern Utah. In S. G. Baines & R. H. Worden (Eds.), *Geological storage of carbon dioxide* (Vol. 233, pp. 43–58). London: The Geological Society of London Special Publication

Sibson, R. H. (2000). Fluid involvement in normal faulting. *Journal of Geodynamics, 29*, 469–499. doi:10.1016/S0264-3707(99)00042-3

Şaroğlu, F., Emre, Ö., & Boray, A., (1987). *Turkey's active faults and earthquakes* (Report No. 5216). General Directorate of Mineral Research and Exploration, Ankara. [in Turkish]

Şaroğlu, F., & Yılmaz, Y. (1986). The geologic evolution and basin models in neotectonic period in east Anatolia. *Bulletin of the Mineral Research and Exploration, 107*, 73–94.

Şengör, A., Özeren, S., Genç, T., & Zor, E. (2003). East Anatolian high plateau as a mantlesupported, north–south shortened domal structure. *Geophysical Research Letters, 30*, 1–12.

Şengör, A. M. C., & Kidd, W. S. F. (1979). Post-collisional tectonics of the Turkish-Iranian plateau and a comparison with Tibet. *Tectonophysics, 55*(3–4), 361–376. doi:10.1016/0040-1951(79)90184-7

Şengör, A. M. C., & Yılmaz, Y. (1981). Tethyan evolution of Turkey: A plate tectonic approach. *Tectonophysics, 75*, 181–190, 193–199, 203–241. doi:10.1016/0040-1951(81)90275-4

Soysal, H., Sipahioğlu, S., Kolcak, D., & Altınok, Y. (1981). *Türkiye ve çevresinin tarihsel deprem katalogu* [The historical earthquake catalog of Turkey and surroundings (TBAK-341)]. Ankara: TUBİTAK.

Tan, O., Tapırdamaz, M. C., & Yörük, A. (2008). The earthquake catalogues for Turkey. *Turkish Journal of Earth Sciences, 17*, 405–418.

Temiz, U., & Eikenberg, J. (2011). U/Th dating of the travertine deposited at transfer zone between two normal Faults and their neotectonic significance: Cambazli fissure ridge travertines (the Gediz Graben-Turkey). *Geodinamica Acta, 24*, 95–105.

Temiz, U., Gökten, E., & Eikenberg, J. (2009). U/Th dating of fissure ridge travertines from the Kirsehir region (Central Anatolia Turkey): Structural relations and implications for the Neotectonic development of the Anatolian block. *Geodinamica Acta, 22*, 201–213. doi:10.3166/ga.22.201-213

Uysal, I, Feng, Y., Zhao, J. X., Altunel, E., Weatherley, D., Karabacak, V., Collerson, K. D. (2007). U-series dating and geochemical tracing of late Quaternary travertine in co-seismic fissures. *Earth and Planetary Science Letters, 257*, 450–462.

Uysal, I. T., Feng, Y., Zhao, J. X., Isik, V., Nuriel, P., & Golding, S. D. (2009). Hydrotermal CO_2 degassing in seismically active zones during the Late Quaternary. *Chemical Geology, 265*, 442–454. doi:10.1016/j.epsl.2007.03.004

Yanık, G., Uz, B., & Esenli, F. (2005, September 21–25). An example of the fissure-ridge type travertineoccurrences: The Cambazli travertine, Turgutlu, west Anatolia. In M. Özkul, S. Yagiz, & B. Jones (Eds.), *Proceedings of 1st International Symposium on Travertine, Denizli, Turkey* (pp. 149–153). Ankara: Kozan Ofset.

Yılmaz, Y. (1971). *Etüde petrographicque et geochronologique de la region de Casa (Partie Meridionale du Masif de Bitlis, Turquie, These de doct 3 cycle)* (p. 230). University Science of Medicine Greonable.

Yılmaz, O. (1975). Casas Region (Bitlis Massif) stratigraphic and petrographic examination of the rocks. *Geological Bulletion of Turkey, 18–1*, 33–40.

Yılmaz, Y., Şaroğlu, F., & Güner, Y. (1987). Initiation of the neomagmatism in East Anatolia. *Tectonophysics, 134*, 177–199. doi:10.1016/0040-1951(87)90256-3